




Cylinder-based Efficient and Robust Registration and Model Fitting of Laser-scanned Point Clouds for As-built Modeling of Piping Systems

Ryota Moritani¹ , Satoshi Kanai² , Hiroaki Date³ , Masahiro Watanabe⁴ ,
Takahiro Nakano⁵  and Yuta Yamauchi⁶ 

¹Hokkaido University, r_moritani@sdm.ssi.ist.hokudai.ac.jp

²Hokkaido University, kanai@ssi.ist.hokudai.ac.jp

³Hokkaido University, hdate@ssi.ist.hokudai.ac.jp

⁴Hitachi, Ltd., masahiro.watanabe.ub@hitachi.com

⁵Hitachi, Ltd., takahiro.nakano.tz@hitachi.com

⁶Hitachi, Ltd., yuta.yamauchi.kj@hitachi.com

Corresponding author: Ryota Moritani, r_moritani@sdm.ssi.ist.hokudai.ac.jp

ABSTRACT

In this work, we improved the efficiency and accuracy of our proposed cylinder-based registration and model fitting method of point clouds by terrestrial laser scanners for the as-built modeling of piping systems. Our algorithm simultaneously calculated the scanner parameters and cylinder parameters to avoid the propagation of registration errors and modeling errors. Coarse registration is performed by finding the alignment of the cylinder axes based on the random sample consensus approach and using a hash table. The efficiency of the coarse registration is improved by introducing a three-dimensional hash table. The fine registration and modeling is performed by minimizing the fitting errors of the cylinders as a nonlinear function of the positional and geometric parameters of scanners and cylinders. An iteratively reweighted least squares method is applied to the fine registration and modeling, leading to improved robustness. Moreover, for the modeling of pipes that are slightly bent due to gravity, incident angle filtering of scanned points and cylinder subdivision of the pipes to be modeled are introduced. The efficiency and robustness of the improved algorithm were compared with the previous approach using both artificial and real point clouds. The effectiveness of incident angle filtering and cylinder subdivision was confirmed. The proposed algorithm achieved the level of cylindrical modeling precision required for the renovation work of piping systems.

Keywords: Laser Scanning, Registration, As-built Modeling, Point Clouds, Piping System, Terrestrial Laser Scanner, Robust Fitting.

DOI: <https://doi.org/10.14733/cadaps.2019.396-412>

1 INTRODUCTION

Recently, aging plant piping systems and the shortening of life cycle have been increasing the frequency of renovation work. In the renovation work where a part of the old piping system are exchanged to the new ones, the constructor can scarcely use the three-dimensional piping models because they are as-planned. Moreover, even if the constructor can use them, the as-built geometries are not often represented precisely in them since the small-scale renovation work is often performed. Therefore, the as-built measurement and modeling are needed to estimate the accurate cylinder parameters right before the renovation work. And the demand for three-dimensional as-built modeling of plant piping systems is currently increasing based on a point cloud captured by a terrestrial laser scanner (TLS) which measures the current environment shapes accurately and efficiently (e.g. [5], [16]). To construct an as-built three-dimensional piping system model based on scanned data, a registration process is needed to align multiple point clouds, including many cylindrical piping objects. The iterative closest point (ICP) [4] algorithm is frequently used to conduct the registration. However, when capturing a cylindrical surface from different scanner positions, the point clouds tend to overlap only in portions with high laser beam incident angles. Therefore, they suffer from a large amount of noise and errors. Thus, as shown in Figure 1(a), the alignment results of ICP include non-negligible errors or fail when the overlap between point clouds is small or absent. Moreover, since cylinder models are fitted to the registered point clouds, the registration error propagates to the model fitting error and results in unacceptable accuracy degradation in the final as-built model.

In our previous study [21] (Figure 1(b)), we proposed a simultaneous cylinder-based registration and model fitting method for the as-built modeling of piping systems. The cylinder-based coarse registration method based on random sample consensus (RANSAC) was also proposed in that study. This method does not necessarily require overlap between point clouds in the registration. The method can also avoid the propagation of errors from registration to cylinder fitting to achieve a highly accurate as-built modeling of piping systems. However, the registration and model fitting of our proposed method [21] has two drawbacks in relation to its efficiency and robustness.

The first drawback concerns the excessively large point clouds measured on a large-scale piping system, which make coarse registration inefficient. The proposed coarse registration in [21] is needed to find the initial scanner positions and the initial corresponding cylinders between several scans, but the processing time increased rapidly as the number of scanners and extracted cylinders increased, e.g., 2.4 h with only two scans and a few hundred cylinders. In case of more practical periodic renovation works, the processing time to build three-dimensional as-built model should finish at least overnight. However, if our previous coarse registration is applied to the large scale plant piping system, the processing time even for coarse alignment would exceed overnight. This inefficiency was due to the many "fake" cylinders that were mistakenly extracted and because the hash table did not fully discriminate corresponding cylinder pairs in the coarse registration.

The second drawback is that the accuracy of registration and modeling sometimes decreases when it is applied to actual point clouds of complex piping systems in real environments. This inaccuracy is due to the non-negligible systematic error of scanned points appearing at large measurement distances and high incident angles. The presence of outlier points on the pipe (measured at T-junctions and flanges) is a further cause of this inaccuracy. The distribution of systematic error and outliers deviates substantially from a normal distribution. Additionally, our previous registration and model fitting using the least squares approach introduced a certain amount of error.

The objective of the present study was to improve the efficiency and accuracy of our proposed cylinder-based registration and model fitting method for the as-built modeling of piping systems. Many cylinder pipes exist in actual piping systems, and the point clouds captured from that environment contain points measured from bent pipes, noise, and outliers. Against such raw point clouds, our proposed method avoids the propagation of registration and modeling error and generates the as-built model of a piping system with high accuracy. As shown in Figure 2, we first

introduced a selective rough cylinder extraction to obtain the cylinder parameters and points really existing on the cylindrical surface and to decrease the number of mistakenly extracted cylinders. Moreover, we devised a three-dimensional hash table to considerably improve the efficiency of coarse registration. Furthermore, we introduced the iteratively reweighted least squares method (IRLSM) to make the fine registration robust against systematic error and outliers. Incident angle filtering and cylinder subdivision were also applied adaptively to the proposed registration process to increase the modeling accuracy of bent pipes. Finally, we evaluated the effectiveness of these improvements through scan simulations and as-built modeling using real point clouds captured from the piping system of a water treatment plant.

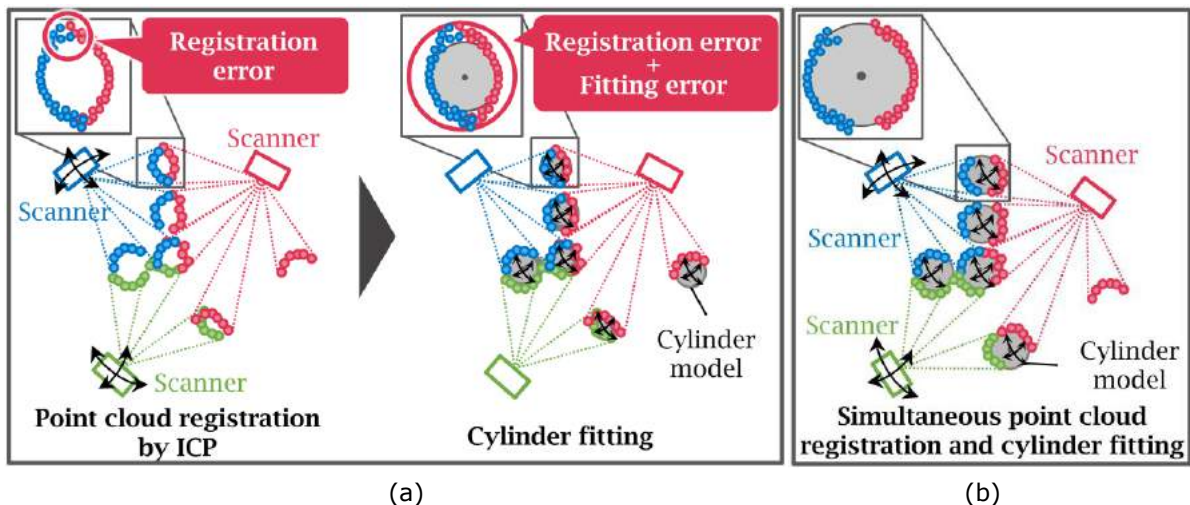


Figure 1: Registration and modeling method of piping system: (a) Conventional ICP-based registration and modeling process; (b) Proposed registration and modeling process.

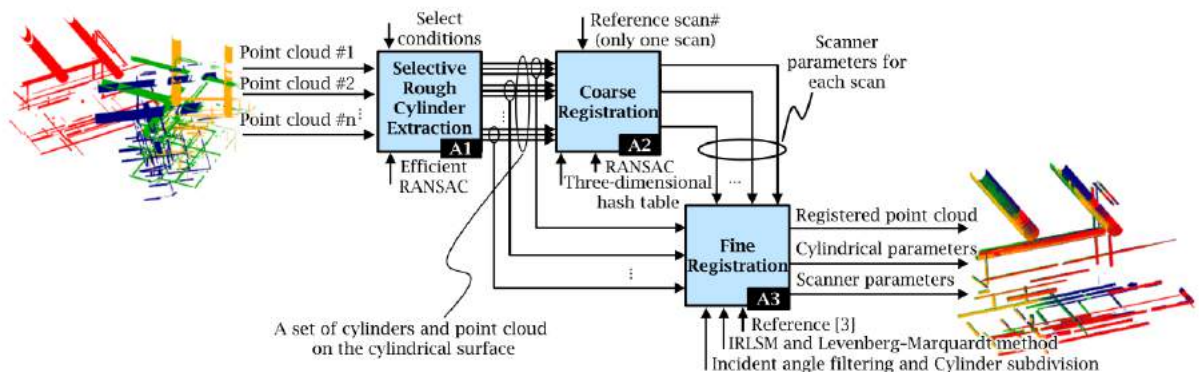


Figure 2: Overview of the proposed fine registration and modeling method.

The rest of this paper is organized as follows. Section 2 discusses previous work and the problems associated with cylindrical modeling and registration for the as-built modeling of piping systems. Selective rough cylinder fitting which is preprocessing of registration is described in Section 3. A coarse registration algorithm based on a three-dimensional hash table is presented in Section

4, and the fine registration and modeling using the IRLSM is described in Section 5. Section 6 presents the efficiency and robustness of the proposed method, which is then applied to point clouds generated from a scan simulation and an actual laser scanning of a water treatment plant piping system. Section 7 concludes the paper.

2 RELATED WORK

Several cylinder modeling methods have been proposed for a three-dimensional as-built model of plant piping systems. These previous studies have extracted the point clouds on pipes from the original scanned point clouds and recognized their cylinder parameters. The estimated normal of each point is projected to the Gaussian sphere, and the point clouds on the cylindrical surface are extracted [10], [19], [23], and [24]. As another approach, the Hough transform and a-priori knowledge of the cylinder parameters are applied to the sliced point clouds [1] for extraction and recognition. Other methods that can recognize straight pipes, elbows, and T-junction pipes have also been proposed [15], [22], and [26].

These studies implicitly assume that the original point clouds have been successfully registered and that sufficient coverage of the points on the cylinders has been also achieved. However, this assumption does not necessarily hold due to the propagation of the registration error to the modeling error (as described above); therefore, the accuracy of the cylinder modeling potentially decreases. Moreover, the accuracy of cylinder modeling depends on the accuracy of the normal vectors of the points. However, it is difficult to estimate an accurate normal vector because a laser scanned point cloud includes a large amount of noise and outliers. In addition, the processing time of the estimation is significantly increased if the normal is estimated with high accuracy for a very large number of point clouds.

From the registration perspective, many marker-less registration methods have been developed. ICP has well-known alignment method of point clouds. Many ICP-variant methods have also been proposed [3], [7], and [30]. In these ICP-based methods, the overlap between multiple point clouds is essential. However, it is sometimes difficult to obtain such an overlap between scans because the pipes in a plant piping system are complexly arranged (tangled) as shown in Figure 3(a), and there is not an enough space to place a TLS (Figure 3(b).) additionally at which the occlusions of point clouds are discovered. Therefore, there are significant restrictions to scanner placement. ICP-based fine registration thus tends to fail when the overlapping point clouds are small or absent.

Moreover, feature-based studies on coarse registration using characteristic objects and shapes in the environment have been proposed: 4-Points Congruent Sets [2] and [27], plane [6], geometric three-dimensional keypoints [8], color information [14], descriptor [16], and image [18] and [28]. Moreover, methods for performing registration after data simplification based on neural networks have recently been developed [12] and [29]. However, these methods aim at coarse registration and have to be followed by fine registration of ICP. As a consequence, the registration error tends to be large in the conventional registration and in the cylinder model fitting of the laser scanned points captured from cylindrical surfaces.

3 SELECTIVE ROUGH CYLINDER FITTING

An overview of the proposed fine registration and modeling method is shown in Figure 2. Our proposed method comprises three steps to construct the as-built model of plant piping system: cylinder rough fitting, coarse registration, and fine registration.

First, we remove point clouds on the floor surface, which occupies most of the raw point cloud P_r^0 (Figure 4(a)) captured by a TLS. The low density portion of the point clouds and outliers is also removed to reduce the processing time of normal estimation and cylinder extraction of the post processing. Under the hypothesis that the z direction of the point clouds measured by a TLS is identical to the upward vertical direction, a histogram of the point cloud distribution in the vertical direction is constructed (Figure 4(b).) and the mode value of the histogram is extracted. We then

remove the point clouds distributed to the z ranges equal to or lower than the mode value as a floor point cloud (Figure 4(c)).

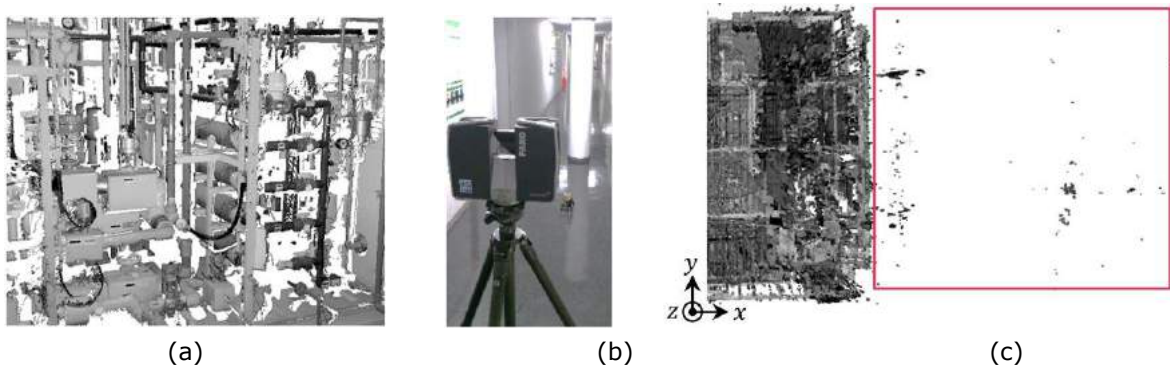


Figure 3: A typical setup: (a) Close-up image of point cloud in a water treatment plant piping system; (b) A typical setup of the scanning by a TLS; (c) Top-down view of point cloud, and a red square represents outliers outside of wall.

First, we remove point clouds on the floor surface, which occupies most of the raw point cloud P_r^0 (Figure 4(a)) captured by a TLS. The low density portion of the point clouds and outliers is also removed to reduce the processing time of normal estimation and cylinder extraction of the post processing. Under the hypothesis that the z direction of the point clouds measured by a TLS is identical to the upward vertical direction, a histogram of the point cloud distribution in the vertical direction is constructed (Figure 4(b).) and the mode value of the histogram is extracted. We then remove the point clouds distributed to the z ranges equal to or lower than the mode value as a floor point cloud (Figure 4(c)).

Next, to remove point clouds with low density, as well as outliers, space subdivision by cell of an Octree data structure is performed for the point cloud P_r^1 which is remained except for points on the floor surfaces. As shown in Figure 4(d)., space in the bounding box of P_r^1 is subdivided into Octree cells. The minimum side length of a cell is 20 mm. A set of points is removed so that the number of point clouds in a cell is less than the threshold τ_{pts} (Figure 4(e).).

The accidental error of the measurements becomes larger as its distance from the scanner becomes larger. Moreover, outliers with extremely long distances are frequently observed due to surface specular reflection or beam splits on object edges (Figure 3(c).). Therefore, a set of points whose distance from the scanner is greater than the threshold τ_d is removed. The point clouds remaining after this outlier removal are denoted as P_r^2 .

Finally, PCA-based normal estimation and Efficient RANSAC [25] are performed to extract the fragments of cylindrical pipe surfaces and their supporting inlier points from P_r^2 . Efficient RANSAC is able to estimate the primitive shapes with high efficiency. However, inappropriate cylinders with very short lengths, or with extremely small or large radii (which do not conform to industry standards), are also extracted by Efficient RANSAC. These inappropriate cylinders should not be applied to the proposed registration and modeling method and should be removed. To this end, as shown in Figure 5., only those cylinders that satisfy the following criteria are selected:

- the number of points on the cylindrical surface is greater than the threshold τ_N ;
- the length of the cylinder is greater than the threshold τ_l [m];
- the radius of the cylinder ranges from $\tau_{r_{min}}$ [m] to $\tau_{r_{max}}$ [m];

- d) the central angle of a circular arc spanned by the projected points is greater than τ_{deg} , where the points on a cylindrical surface are projected to a plane perpendicular to the cylinder axis.

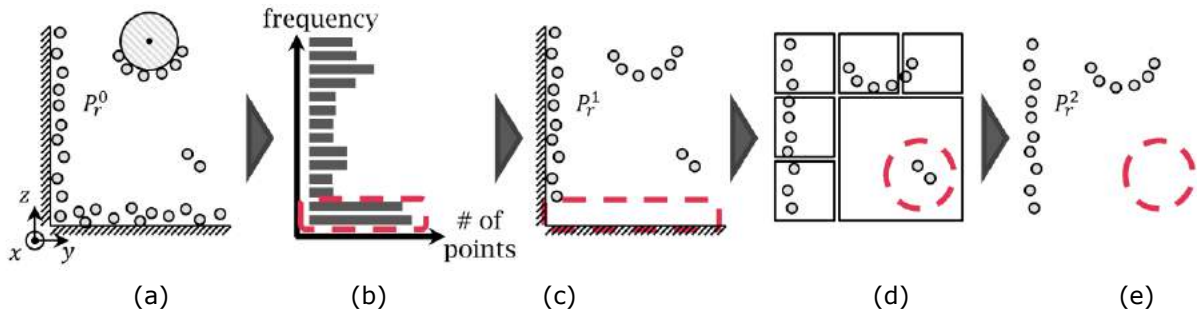


Figure 4: Removal of the point cloud on the floor and with low density: (a) The original point cloud; (b) The histogram of the point cloud distribution; (c) The point cloud after removal of points on the floor; (d) Space subdivision of (c); (e) The point cloud after removal of low density point clouds.

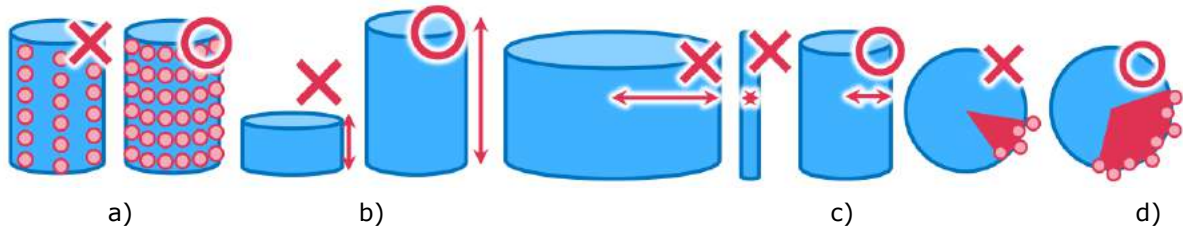


Figure 5: Cylinder selective conditions: a) The number of points; b) The length of cylinder; c) The radius of cylinder; d) The central angle of a circular arc.

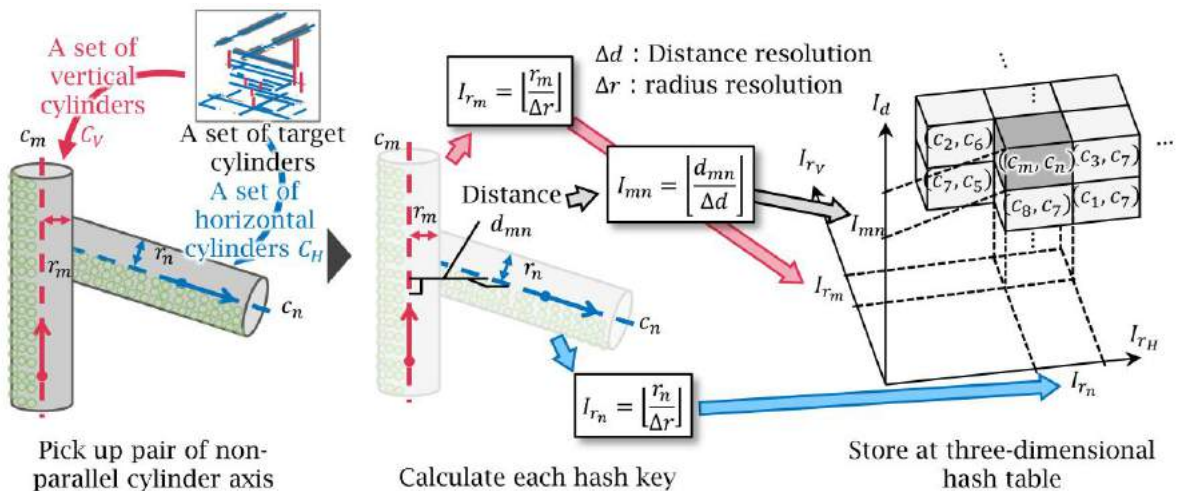


Figure 6: Construction of a three-dimensional cylinder pair hash table.

5 CYLINDER-BASED SIMULTANEOUS FINE SCAN REGISTRATION AND MODEL FITTING BASED ON IRLSM

5.1 Principle of Simultaneous Registration and Model Fitting

As shown in Figure 7, the positional and geometric parameters of scanners \mathbf{x}_j^{Reg} and cylinders \mathbf{x}_k^{Cyl} were calculated simultaneously by minimizing the fitting error along the orthogonal direction from the point clouds to the analytic cylinder surfaces. This minimization was formulated as follows:

$$\underset{\{\mathbf{x}_j^{Reg}\}, \{\mathbf{x}_k^{Cyl}\}}{\text{minimize}} \sum_{j \in B - \{t_0\}} \sum_{k \in C} \sum_{i \in P_k} w \left(D_{jk} \left(i; \mathbf{x}_j^{Reg}, \mathbf{x}_k^{Cyl} \right) \right) \left[D_{jk} \left(i; \mathbf{x}_j^{Reg}, \mathbf{x}_k^{Cyl} \right) \right]^2 \quad (1)$$

where B is a set of scanners, t_0 is a scanner at a reference (fixed) location, and C is a set of uniquely identified cylinders in all scans $\{s^j\}$. P_k denotes a set of scanned points placed on cylinder k and \mathbf{x}_k^{Cyl} are the model parameters of cylinder k . \mathbf{x}_j^{Reg} denotes the registration parameters of scanner j . $D_{jk}(i; \mathbf{x}_j^{Reg}, \mathbf{x}_k^{Cyl})$ denotes the fitting error function of scanned point i from cylinder k located at \mathbf{x}_k^{Cyl} when a point i is captured by scanner j located at \mathbf{x}_j^{Reg} . $w(\cdot)$ is the weight function at point i , and the fitting error is employed as the variable of the $w(\cdot)$, its selection will be discussed in the next section. This simultaneous adjustment of \mathbf{x}_j^{Reg} and \mathbf{x}_k^{Cyl} prevented the alignment error of the fine registration from propagating through the following model fitting, and helped preserve the modeling accuracy of the piping system.

The error function $D_{jk}(i)$ evaluated the squared orthogonal distance of a point from its corresponding cylindrical surface. To simplify the evaluation, we first classified the direction of the cylinder axis obtained from the course registration into one of three dominant orthogonal axial directions (X_0 , Y_0 , or Z_0) in the world coordinate system Σ_0 , as proposed in [9]. For example, when the cylinder axis is nearly parallel to the Z_0 axis, the error function $D_{jk}(i)$ is defined by Eqs. (2) and (3):

$$D_{jk}(i; \mathbf{x}_j^{Reg}, \mathbf{x}_k^{Cyl}) = \sqrt{p_{ix}'^2 + p_{iy}'^2 - r_k^2} \quad (2)$$

$$\mathbf{p}_i' = \mathbf{R}(\Phi_k) \mathbf{R}(\Omega_k) \{\mathbf{p}_i - \mathbf{q}_k\} \quad (3)$$

where $\mathbf{p}_i = [p_{ix}, p_{iy}, p_{iz}]^t$ and $\mathbf{p}_i' = [p_{ix}', p_{iy}', p_{iz}']^t$ are the positions of a point i w.r.t. Σ_0 and a local coordinate system Σ_k^C fixed on cylinder k , with radius $r_k (\in \mathbf{x}_k^{Cyl})$, respectively, i.e., on the plane perpendicular to the cylinder axis, \mathbf{p}_i' represents the positions of a projected point, and $D_{jk}(i)$ evaluates the radical fitting error of the sectional circle of the cylinder. $\mathbf{q}_k = [q_{kx}, q_{ky}, 0]^t (\in \mathbf{x}_k^{Cyl})$ is the intersection point between the cylinder axis and the X_0Y_0 plane w.r.t. Σ_0 , $\mathbf{R}(\cdot)$ is a 3×3 rotation matrix, and $\Omega_k (\in \mathbf{x}_k^{Cyl})$ and $\Phi_k (\in \mathbf{x}_k^{Cyl})$ are the Cardan angles for the rotation about the X_0 and Y_0 axis, respectively. Angles Ω_k and Φ_k specify the axial orientation of cylinder k . In this case, the controlled valuables are represented as $\mathbf{x}_j^{Reg} = [X_{S_j}, Y_{S_j}, Z_{S_j}, \omega_j, \phi_j, \kappa_j]$ and $\mathbf{x}_k^{Cyl} = [q_{kx}, q_{ky}, \Omega_k, \Phi_k, r_k]$, here, X_{S_j}, Y_{S_j} and Z_{S_j} denotes positional parameters and $\omega_j, \phi_j, \kappa_j$ is rotational (Cardan) angles of scanner j , respectively. The cylinder axes nearly parallel to the X_0 or Y_0 axis are formulated in a similar manner.

The minimization problem of Eqn. (1) becomes nonlinear; however, we can derive the optimal solution of \mathbf{x}_j^{Reg} and \mathbf{x}_k^{Cyl} by starting from the initial values obtained from the coarse registration and using the Levenberg-Marquardt method.

5.2 Optimization Process using the Iteratively Reweighted Least Squares Method

We introduce the iteratively reweighted least squares method (IRLSM) instead of the least squares method (LSM) in order to solve the minimization problem expressed by Eqn. (1). Compared with the

LSM, the IRLSM is more robust against systematic error and outliers because a weight function depending on the error amount is assigned.

In this study, as shown in Figure 8, we tested the following three types of weight function, as given by Eqs. (4), (5), and (6):

$$\text{Fair:} \quad w(e_i) = 1/(1 + |e_i|/c) \quad (4)$$

$$\text{Huber:} \quad w(e_i) = \begin{cases} 1 & |e_i| \leq c \\ c/|e_i| & |e_i| > c \end{cases} \quad (5)$$

$$\text{Tukey:} \quad w(e_i) = \begin{cases} [1 - (e_i/c)^2]^2 & |e_i| \leq c \\ 0 & |e_i| > c \end{cases} \quad (6)$$

where c is the parameter controlling the support range of each weight function. We adopted the residual error $D_{jk}(i)$ of the scanned point i as the weight variable e_i . The weight value of Eqn. (4) was halved if $e_i = c$. In the case of Eqn. (5), if $|e_i| \leq c$, the weight value was 1, if $|e_i| > c$, the weight value decreased gradually depending on the value of c . However, the weight never converged to zero. On the other hand, Eqn. (6) decreased to zero if $|e_i| > c$, and was highly dependent on the initial values. However, the outlier was rejected completely. The accuracy of the IRLSM depended on correctly choosing the control parameter c . We adopted a normalized median absolute distribution about the median (MADN) [20] of $\{e_i\}$ as c . MADN is expressed by Eqs. (7) and (8):

$$\text{MADN}(e) = \text{MAD}(e)/0.6745 \quad (7)$$

$$\text{MAD}(e) = \text{MAD}(e_1, e_2, \dots, e_n) = \text{Med}\{|e - \text{Med}(e)|\} \quad (8)$$

In comparison with the standard deviation, the median absolute distribution about the median (MAD) was less affected by large outliers owing to the use of the median of $\{e_i\}$. Therefore, MADN could provide a robust estimator alternative to the standard deviation. The value of MADN decreased automatically because it was recalculated at each IRLSM iteration.

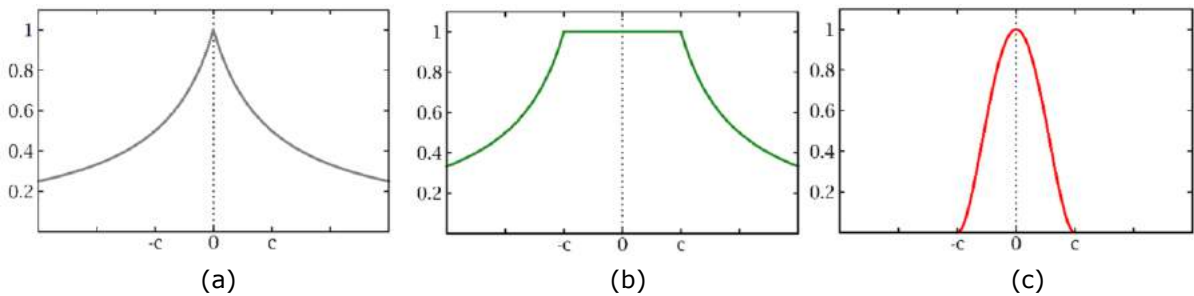


Figure 8: Weight functions: (a) Fair function; (b) Huber function; (c) Tukey function.

5.3 Incident Angle Filtering and Cylinder Subdivision

In our previous study [21], we showed that the systematic and accidental error of laser scanned point clouds greatly depends on the incident angle of the laser beam. Therefore, we opt to remove point clouds with an incident angle equal to or larger than τ_α [°] and not apply them to the minimization processing of fine registration. Points with large incident angles often appear in the overlap portions between scans. Therefore, in the previous ICP-based registration method, it was difficult to filter out the points with a large incident angle because the registration ICP requires the overlapped points. However, our proposed method can align the point clouds even if incident angle filtering is applied and overlap between point clouds is small or absent.

Moreover, our approach is designed for simultaneous fine registration and modeling as it uses straight cylindrical pipes as markers. However, it is sometimes difficult to apply the algorithm to the real point cloud when these pipes are slightly bent due to the influence of gravity and/or fixture constraints at the pipe's ends. To overcome this issue and to model bent pipes more accurately as cylinders, if an original cylindrical pipe has a length equal to or longer than the threshold τ_{ch} [m], it is equally divided into n pieces of shorter cylinders along its axis.

6 EVALUATION OF MODELING ACCURACIES AND EFFICIENCIES

6.1 Modeling Accuracies of Point Clouds Generated from Scan Simulations

We compared the cylinder modeling accuracy achieved using the proposed IRLSM-based method without cylinder subdivision and incident angle filtering under different weight function settings with that achieved by ICP and our previous LSM-based approach [21]. First, we generated artificial point clouds from the CAD model of a piping system, where a Gaussian-type measurement error was superimposed along the laser beam direction using scan simulation software. Three point clouds with a total of 5.65 million points were generated from three different scanner positions. The CAD model of the simple piping system ($10\text{ m} \times 15\text{ m} \times 8\text{ m}$) is shown in Figure 9. Table 1 shows the thresholds used in the modeling. Then, the three point clouds were aligned by the proposed coarse registration method using 10 manually selected cylinders. Finally, fine registration and model fitting were performed under 12 different conditions, as shown in Table 2. The fine registration of condition I was performed by our previous LSM-based registration and modeling method. The fine registration of condition II was executed by built-in ICP-based registration functions using freely available software [11]. A commercial software package was used for condition III [13]. For conditions II and III, least-squared fitting was used for modeling of the final cylinder. For conditions IV–VI, the proposed fine registration and modeling method using the IRLSM, which is expressed by Eqn. (4), were applied with different control parameter settings for the weight function ($1 \times \text{MADN}$, $3 \times \text{MADN}$, and $6 \times \text{MADN}$). Conditions VII–IX using the IRLSM expressed by Eqn. (5), and conditions X–XII using the IRLSM expressed by Eqn. (6), were applied with control parameter settings similar to those of conditions IV–VI.

Table 3 shows the distributions of distance error E_d , angle error E_a , and cylinder radius error E_r , between the two cylinder axes after fine registration. Their exact values were provided by the original CAD model. Methods I and IV–XII clearly yielded more accurate modeling results in comparison with the conventional ICP-based method (conditions II and III). In particular, in condition XII, the error was reduced to a submillimeter order, which was approximately one-tenth of the errors under conditions II and III. Therefore, it is evident that condition XII achieved the best accuracy. The processing time under condition I was approximately 54 s, whereas that under condition XII was 142 s.

Finally, the relationship between the processing time and the number of input point clouds was investigated. For this purpose, the artificial scanned point clouds with different point-to-point interval settings were scanned using simulation software. The point-to-point interval was adjusted from 3 mm to 25 mm at 10 m, as shown in Table 4. The proposed fine registration and modeling methods were used under condition I. As shown in Figure 10., the processing time linearly increased with the number of point clouds. Moreover, even if the number of point clouds was not changed, the processing time increased when the number of scanner positions and cylinders to be modeled increased because the processing time of minimization in Eqn. (1) is positively correlated with the number of variables.

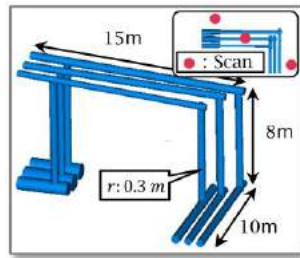


Figure 9: CAD model of simple piping system.

The number of points in a cell τ_{pts}	50
Distance τ_d for removal [m]	30
The number of points τ_N	2500
The length of the cylinder τ_l [m]	0.5
The minimum radius of the cylinder $\tau_{r_{min}}$ [m]	0.03
The maximum radius of the cylinder $\tau_{r_{max}}$ [m]	1.0
The central angle τ_{deg} [°]	120

Table 1: Threshold values used in the evaluation of modeling accuracies and efficiencies.

	Condition											
	I	II	III	IV	V	VI	VII	VIII	IX	X	XI	XII
Registration method	LSM	Free software	Commercial software	IRLSM using Eqn. (4)			IRLSM using Eqn. (5)			IRLSM using Eqn. (6)		
Modeling method		LS Fitting										
Control parameter $c = \text{MADN}$	-	-	-	× 1	× 3	× 6	× 1	× 3	× 6	× 1	× 3	× 6

Table 2: Fine registration conditions and value of control parameters.

		Condition											
		I	II	III	IV	V	VI	VII	VIII	IX	X	XI	XII
Distance error E_d [mm]	Average	0.38	2.72	1.51	0.28	0.33	0.37	0.17	0.11	0.21	0.86	0.15	0.04
	Maximum	1.67	6.31	3.04	0.64	0.91	1.10	0.26	0.22	0.47	1.70	0.24	0.06
Angle error E_α [deg]	Average	0.021	0.080	0.047	0.004	0.006	0.008	0.001	0.002	0.006	0.005	0.000	0.001
	Maximum	0.037	0.239	0.110	0.008	0.013	0.018	0.001	0.006	0.014	0.011	0.001	0.001
Absolute value of radius error E_r [mm]	Average	0.49	0.48	0.66	0.10	0.13	0.15	0.07	0.08	0.12	0.12	0.07	0.06
	Maximum	1.89	1.62	2.20	0.32	0.49	0.62	0.15	0.23	0.54	0.26	0.15	0.13

Table 3: Average errors and maximum values of errors after fine registration (bold indicates best values).

6.2 Efficiencies for Real Point Clouds of a Water Treatment Plant Piping System

The proposed method was then applied to real, large-scale laser scanned point clouds of a small water treatment plant piping system, as shown in Figure 11, and its efficiency was verified. First, the proposed coarse and fine registration methods without cylinder subdivision and incident angle filtering under condition XII were applied to real point clouds, and their efficiencies were compared with that of the conventional method. The real point clouds of a real water treatment plant piping system ($15m \times 10m \times 5m$), with a total of 4.37 million points, were captured by TLS (Faro Focus 3D) from four scanner positions. Selective rough cylinder extraction was applied to the point clouds of each of the four scans in order to identify approximately 100 cylinder fragments in each scan, as shown in Figure 11(a). The point clouds were then aligned by coarse registration. Coarse registration with the one-dimensional hash table [21] took 7.7 min, whereas with the three-dimensional hash table, it took only 0.7 min. The maximum number of hash key collisions also decreased from 662 to 162. Moreover, the proposed IRSLM-based fine registration and modeling methods under condition XII were applied to the point cloud after coarse registration, obtaining the final result shown in Figure 11(b). The fine registration and modeling under condition XII took 84 sec. As shown in Figure 11(b), visual inspection confirmed that fine registration was successfully completed.

The PtoP interval between the scanned points @10m [mm]	The number of points [Million points]
3.068	22.95
6.136	5.65
7.670	3.67
12.282	1.43
15.340	0.91
24.544	0.33

Table 4: Interval and number of points.

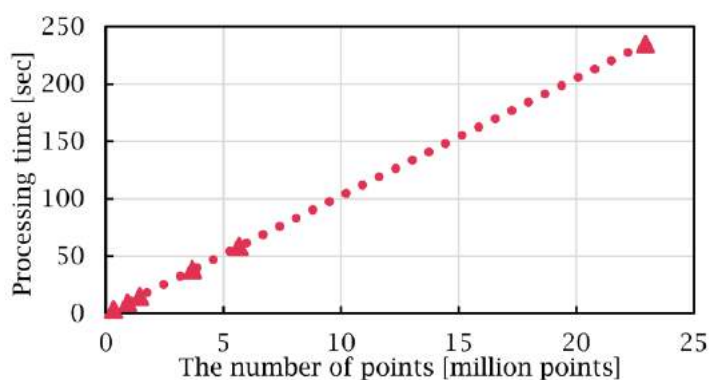


Figure 10: Processing time at each interval.

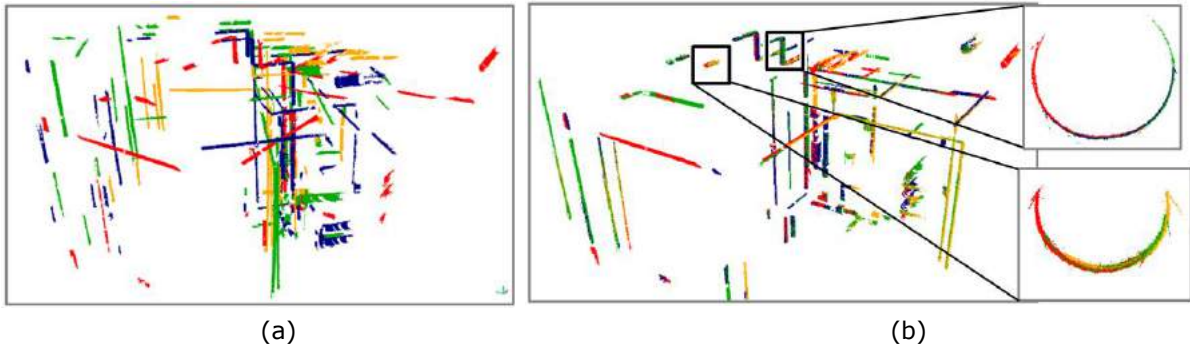


Figure 11: Scanned point clouds before registration and after fine registration under condition XII: (a) Cylinder fragment point clouds before registration; (b) Scanned point clouds after fine registration under condition XII. The red point cloud is a reference cloud, to which the other point clouds are aligned.

Next, we investigated the accuracy of the proposed fine registration in the real environment as well as the effectiveness of cylinder subdivision and incident angle filtering. The proposed coarse and fine registration methods with cylinder subdivision and incident angle filtering under condition XII were applied to the same environment described above. The 12 scanned point clouds with a total of 16.46 million points were captured by TLS. The number of cylinder subdivisions was set to $n = 2$, the length threshold to $\tau_{ch} = 1.5$ [m], and the incident angle threshold to $\tau_{\alpha} = 60$ [°]. Figure 12(a) and (b) show the results. The processing time of fine registration and modeling was 9.3 min. As shown in Figure 12(c) and (d), when the fine registration and modeling without cylinder subdivision and incident angle filtering were applied to bent pipes, the fitting error became very large. On the contrary, as shown in Figure 12(e) and (f), the registration and modeling with cylinder subdivision and incident angle could fit the cylinder model to the bent pipes more accurately than those of subdivision. The average of the fitting error of all cylinders decreased from 5.0 mm to 3.3 mm.

As shown in Figure 13, to evaluate the registration accuracy of the proposed method, we first selected an arbitrary pair of raw point clouds and extracted the well-measured points existing on a plane of factory equipment from each raw point cloud. Then, the least-square plane was fitted to the point cloud on the plane. This allowed us to regard the distance from one plane to the other as the registration error. The average errors of three planer point cloud pairs when three raw point cloud pairs were selected are summarized in Table 5. As a result, the maximum registration error between planes was below 3 mm despite the fact that our method only uses cylinders for the registration. Moreover, we confirmed the accuracy and effectiveness of the proposed registration method for the laser scanned point clouds in the real environment.

Since the reference CAD model of this plant was not available, we compared the distance between two cylinder axes calculated by the proposed method with that between points on the pipe surfaces existing in a single point cloud, as shown in Figure 14. We first selected an arbitrary pair of modeled pipes and calculated the distance between them using their cylinder axes and radii values, which were obtained by the proposed method. Secondly, in a single scanned point cloud, approximately the same line as the distance between two modeled pipes was drawn interactively and two measured points on each pipe were also selected interactively. Then, the distance between the two points was assumed to be a true value. Finally, we compared the error between the two distances for eight pairs of pipes (the distances between cylinders approximately distributed from 3 m to 6 m). As shown in Tab. 5, the average distance error was 1.6 mm and the maximum error was 4.0 mm. From this result, we confirmed that the accuracy of the cylindrical modeling of the proposed method in the real environment fully satisfied the precision necessary for the as-built modeling of pipes in cases where renovation work is required.

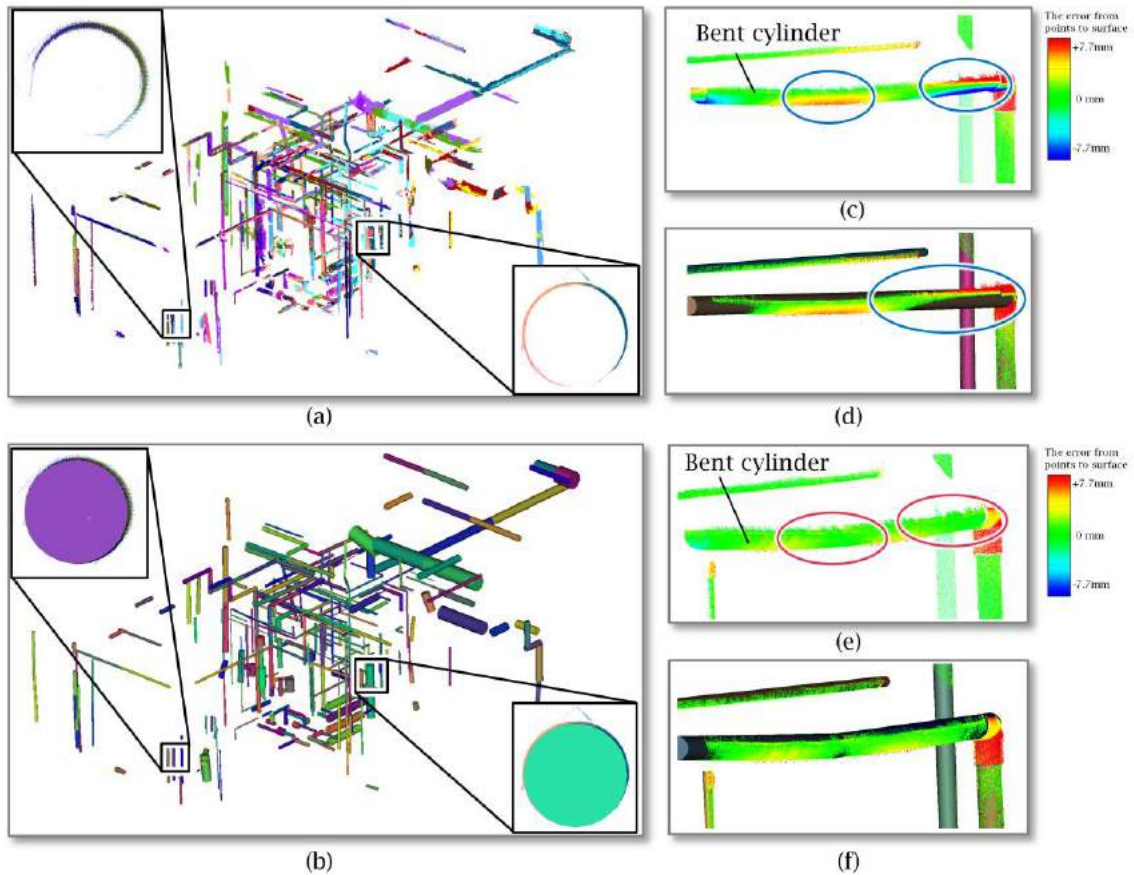


Figure 12: Results of fine registration and cylinder modeling in the proposed method with cylinder division and incident angle filtering under condition XII: (a) Fine registration result with cylinder division and incident angle; (b) Cylinder modeling result with cylinder division and incident angle; (c) and (d) Errors from points to cylindrical surface for registration and modeling without cylinder subdivision and incident angle, respectively; (e) and (f) Errors from points to cylindrical surface after registration and modeling with cylinder subdivision and incident angle, respectively.

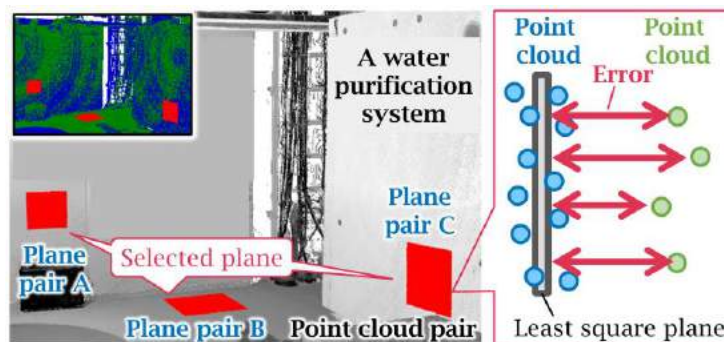


Figure 13: Overview of fine registration evaluation method and example of the selected point cloud pair.

Point cloud pair	Plane pair		
	A	B	C
I	0.9 mm	1.1 mm	0.9 mm
II	0.7 mm	3.0 mm	0.9 mm
III	0.6 mm	0.9 mm	0.5 mm

Table 5: The average of distance error between point clouds in fine registration.

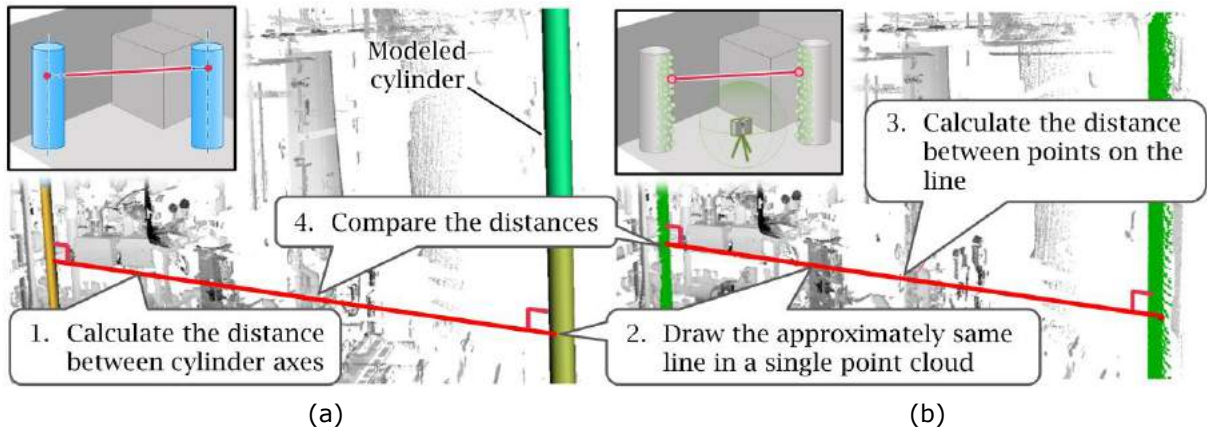


Figure 14: Overview of cylinder modeling evaluation method: (a) Modeling result by the proposed method; (b) Single scan point cloud.

7 CONCLUSIONS

The efficiency and accuracy of a simultaneous cylinder-based registration and model fitting method was improved with regard to the as-built modeling of piping systems. A three-dimensional hash table was introduced to the coarse registration. The IRLSM-based fine registration and model fitting methods were robust against systematic error and outliers. The simulation results obtained in this study confirmed that the modeling accuracy achieved by the proposed IRLSM-based approach clearly outperformed the previous LSM-based and ICP-based approaches with regard to modeling accuracy. In a real water plant piping system, the three-dimensional hash table yielded highly efficient coarse registration. Furthermore, incident angle filtering and cylinder subdivision were applied to produce more accurate cylinder modeling of slightly bent pipes. For the proposed method, we confirmed that the fitting error of the cylinder to the laser scanned point clouds of plant piping systems clearly decreased when compared with our previous method. Through the verification of the large-scale point clouds of a few factories, we also confirmed that the proposed method attained the registration and modeling accuracy required for piping systems renovation work.

In future work, the processing time of fine registration will be decreased by subsampling the points on the cylindrical surfaces based on radius and/or measurement distance. By using subsampling, the number of points of each cylinder can be uniformly distributed, and there is a potential to further decrease the error of the registration and modeling.

Ryota Moritani, <http://orcid.org/0000-0001-5051-7890>

Satoshi Kanai, <http://orcid.org/0000-0003-3570-1782>

Hiroaki Date, <http://orcid.org/0000-0002-6189-2044>

Masahiro Watanabe, <http://orcid.org/0000-0003-2486-7648>

Takahiro Nakano, <http://orcid.org/0000-0002-6946-5629>
 Yuta Yamauchi, <http://orcid.org/0000-0003-0289-8398>

REFERENCES

- [1] Ahmed, M. F.; Haas, C. T.; Haas, R.: Automatic detection of cylindrical objects in built facilities, *Journal of Computing in Civil Engineering*, 28(3), 2014. [https://doi.org/10.1061/\(ASCE\)CP.1943-5487.0000329](https://doi.org/10.1061/(ASCE)CP.1943-5487.0000329)
- [2] Aiger, D.; Mitra, N. J.; Cohen-Or, D.: 4-points congruent sets for robust pairwise surface registration, *ACM Transactions on Graphics (TOG)*, 27(3), 2008, 85:1–85:10. <https://doi.org/10.1145/1399504.1360684>
- [3] Bae, K. H.; Lichti, D. D.: A method for automated registration of unorganised point clouds, *ISPRS Journal of Photogrammetry and Remote Sensing*, 63(1), 2008, 36–54. <https://doi.org/10.1016/j.isprsjprs.2007.05.012>
- [4] Besl, P. J.; McKay, N. D.: A Method for Registration of 3-D Shapes, *IEEE Transactions on Pattern Analysis and Machine Intelligence*, 14(2), 1992, 239–256. <http://doi.org/10.1109/34.121791>
- [5] Bey, A.; Chaine, R.; Marc, R.; Thibault, G.; Akkouche, S.: Reconstruction of Consistent 3d CAD Models from Point Cloud Data Using a Priori CAD Models, *ISPRS - International Archives of the Photogrammetry, Remote Sensing and Spatial Information Sciences*, XXXVIII-5/W12, 2011, 289–294, <https://doi.org/10.5194/isprsjprs-XXXVIII-5-W12-289-2011>
- [6] Bosché, F.: Plane-based registration of construction laser scans with 3D/4D building models, *Advanced Engineering Informatics*, 26(1), 2012, 90–102. <https://doi.org/10.1016/j.aei.2011.08.009>
- [7] Bouaziz, S.; Tagliasacchi, A.; Pauly, M.: Sparse iterative closest point, *Proceedings of the Eleventh Eurographics/ACMSIGGRAPH Symposium on Geometry Processing*, 32(5), 2013, 113–123. <http://dx.doi.org/10.1111/cgf.12178>
- [8] Bueno, M.; González-Jorge, H.; Martínez-Sánchez, J.; Lorenzo, H.: Automatic point cloud coarse registration using geometric keypoint descriptors for indoor scenes, *Automation in Construction*, 81, 2017, 134–148. <https://doi.org/10.1016/j.autcon.2017.06.016>
- [9] Chan, T.O.; Lichti, D.D.; Belton, D.: A rigorous cylinder-based self-calibration approach for terrestrial laser scanners, *ISPRS Journal of Photogrammetry and Remote Sensing*, 99, 2015, 84–99. <https://doi.org/10.1016/j.isprsjprs.2014.11.003>
- [10] Chaperon, T.; Goulette, F.: Extracting cylinders in full 3D data using a random sampling method and the Gaussian image, in *Proceedings of the Vision Modeling and Visualization Conference 2001*, 35–42, 2001.
- [11] Cloud-Compare. <http://www.danielgm.net/cc/>
- [12] Elbaz, G.; Avraham, T.; Fischer, A.: 3D point cloud registration for localization using a deep neural network auto-encoder, *IEEE Conference on Computer Vision and Pattern Recognition (CVPR)*, 2017, 2472–2481. <https://doi.org/10.1109/CVPR.2017.265>
- [13] Geomagic-Wrap. <https://www.3dsystems.com/software/geomagic-wrap>, 3D SYSTEMS
- [14] Gómez-García-Bermejo, J.; Zalama, E.; Feliz, R.: Automated registration of 3D scans using geometric features and normalized color data, *Computer-Aided Civil and Infrastructure Engineering*, 28(2), 2013, 98–111. <https://doi.org/10.1111/j.1467-8667.2012.00785.x>
- [15] Kawashima, K.; Kanai, S.; Date, H.: As-built modeling of piping system from terrestrial laser-scanned point clouds using normal-based region growing, *Journal of Computational Design and Engineering*, 1(1), 2014, 13–26. <https://doi.org/10.7315/JCDE.2014.002>
- [16] Lee, J.; Son, H.; Kim, C.; Kim, C.: Skeleton-based 3D reconstruction of as-built pipelines from laser-scan data, *Automation in Construction*, 35, 2013, 199–207. <https://doi.org/10.1016/j.autcon.2013.05.009>
- [17] Lei, H.; Jiang, G.; Quan, L.: Fast Descriptors and Correspondence Propagation for Robust Global Point Cloud Registration, in *IEEE Transactions on Image Processing*, 26(8), 2017, 3614–3623. <https://doi.org/10.1109/TIP.2017.2700727>

- [18] Lin, C. C.; Tai, Y. C.; Lee, J. J.; Chen, Y. S.: A novel point cloud registration using 2D image features, *EURASIP Journal on Advances in Signal Processing*, 2017(1), 2017. <https://doi.org/10.1186/s13634-016-0435-y>
- [19] Liu, Y. J.; Zhang, J. B.; Hou J. C.; Ren J. C.; Tang W. Q.: Cylinder detection in large-scale point cloud of pipeline plant, *IEEE Transactions on Visualization and Computer Graphics*, 19(10), 2013, 1700–1707. <http://doi.org/10.1109/TVCG.2013.74>
- [20] Maronna, R.A.; Martin, R.D.; Yohai, V.J.: *Robust Statistics*, John Wiley & Sons, Ltd, 2006, 1–16. <http://dx.doi.org/10.1002/0470010940.ch1>
- [21] Moritani, R.; Kanai, S.; Date, H.; Watanabe, M.; Nakano, T.; Yamauchi, Y.: cylinder-based simultaneous registration and model fitting of laser-scanned point clouds for accurate as-built modeling of plant piping systems, *Computer-Aided Design and Applications*, 15(5), 2018, 720–733. <https://doi.org/10.1080/16864360.2018.1441239>
- [22] Patil, A. K.; Holi, P.; Lee, S. K.; Chai, Y. H.: An adaptive approach for the reconstruction and modeling of as-built 3D pipelines from point clouds, *Automation in Construction*, 75, 2017, 65–78. <https://doi.org/10.1016/j.autcon.2016.12.002>
- [23] Qiu, R.; Zhou, Q.; Neumann, U.: Pipe-run extraction and reconstruction from point clouds, *Computer Vision - ECCV 2014*, III, 2014, 17–30. https://doi.org/10.1007/978-3-319-10578-9_2
- [24] Rabbani, T.; Heuvel, F. V. D.: Efficient Hough transform for automatic detection of cylinders in point clouds, *ISPRS Workshop Laser Scanning*, 3, 2005, 60–65.
- [25] Schnabel, R.; Wahl, R.; Klein, R.: Efficient RANSAC for point-cloud shape detection, *Computer Graphics Forum*, 26(2), 2007, 214–226. <http://dx.doi.org/10.1111/j.1467-8659.2007.01016.x>
- [26] Son, H.; Kim, C.: Automatic segmentation and 3D modeling of pipelines into constituent parts from laser-scan data of the built environment, *Automation in Construction*, 68, 2015, 203–211. <https://doi.org/10.1016/j.autcon.2016.05.010>
- [27] Theiler, P. W.; Wegner, J. D.; Schindler, K.: Keypoint-based 4-points congruent sets–automated marker-less registration of laser scans, *ISPRS Journal of Photogrammetry and Remote Sensing*, 96, 2014, 149–163. <https://doi.org/10.1016/j.isprsjprs.2014.06.015>
- [28] Weinmann, M.; Weinmann, M.; Hinz, S.; Jutzi, B.: Fast and automatic image-based registration of TLS data, *ISPRS Journal of Photogrammetry and Remote Sensing*, 66(6), 2011, S62–S70. <https://doi.org/10.1016/j.isprsjprs.2011.09.010>
- [29] Xin, M.; Li, B.; Yan, X.; Chen, L.; Wei, X.: A robust cloud registration method based on redundant data reduction using backpropagation neural network and shift window, *Review of Scientific Instruments*, 89(2), 2018. <https://doi.org/10.1063/1.4996628>
- [30] Yang, J.; Li, H.; Jia, Y.: Go-ICP: Solving 3D registration efficiently and globally optimally, 2013 *IEEE International Conference on Computer Vision*, 2013, 1457–1464. <https://doi.org/10.1109/ICCV.2013.184>